A&A 564, A138 (2014)
DOI: 10.1051/0004-6361/201323098

Astronomy & Astrophysics

WINGS Data Release: a database of galaxies in nearby clusters

A. Moretti[1,2], B. M. Poggianti[2], G. Fasano[2], D. Bettoni[2], M. D'Onofrio[1], J. Fritz[3], A. Cava[4], J. Varela[5], B. Vulcani[6], M. Gullieuszik[2], W. J. Couch[7], A. Omizzolo[2], T. Valentinuzzi[1], A. Dressler[8], M. Moles[5], P. Kjærgaard[9], R. Smareglia[10], and M. Molinaro[10]

[1] University of Padova, Department of Physics and Astronomy "G. Galilei", Vicolo dell'Osservatorio, 2, 35122 Padova, Italy
e-mail: alessia.moretti@oapd.inaf.it
[2] INAF – Osservatorio Astronomico di Padova, Vicolo dell'Osservatorio, 5, 35122 Padova, Italy
[3] Sterrenkundig Observatorium Vakgroep Fysica en Sterrenkunde Universiteit Gent, Krijgslaan 281, S9 9000 Gent, Belgium
[4] Observatoire de Genève, Université de Genève, 51 Ch. des Maillettes, 1290 Versoix, Switzerland
[5] Centro de Estudios de Fisica del Cosmos de Aragon, Plaza San Juan, 1, 44001 Teruel, Spain
[6] Kavli Institute for the Physics and Mathematics of the Universe (WPI), Todai Institutes for Advanced Study, the University of Tokyo, 277-8582 Kashiwa, Japan
[7] Australian Astronomical Observatory, PO Box 915, NSW 1670 North Ryde, Australia
[8] Carnegie Observatories, 813 Santa Barbara Street, Pasadena CA 91101, USA
[9] Niels Bohr Institute, Juliane Maries Vej 30, 2100 Copenhagen, Denmark
[10] INAF – Osservatorio Astronomico di Trieste, via G.B. Tiepolo 11, Trieste, Italy

Received 21 November 2013 / Accepted 3 March 2014

ABSTRACT

Context. To effectively investigate galaxy formation and evolution, it is of paramount importance to exploit homogeneous data for large samples of galaxies in different environments.
Aims. The WIde-field Nearby Galaxy-cluster Survey (WINGS) project aim is to evaluate physical properties of galaxies in a complete sample of low redshift clusters to be used as reference sample for evolutionary studies. The WINGS survey is still ongoing and the original dataset will be enlarged with new observations. This paper presents the entire collection of WINGS measurements obtained so far.
Methods. We decided to make use of the Virtual Observatory (VO) tools to share the WINGS database (that will be updated regularly) with the community. In the database each object has one unique identification (WINGSID). Each subset of estimated properties is accessible using a cone search (including wide-field images).
Results. We provide the scientific community with the entire set of wide-field images. Furthermore, the published database contains photometry of 759 024 objects and surface brightness analysis for 42 275 and 41 463 galaxies in the V and B band, respectively. The completeness depends on the image quality, and on the cluster redshift, reaching on average 90% at $V \lesssim 21.7$. Near-infrared photometric catalogs for 26 (in K) and 19 (in J) clusters are part of the database and the number of sources is 962 344 in K and 628 813 in J. Here again the completeness depends on the data quality, but it is on average higher than 90% for $J \lesssim 20.5$ and $K \lesssim 19.4$. The IR subsample with a Sersic fit comprises 71 687 objects. A morphological classification is available for 39 923 galaxies. We publish spectroscopic data, including 6132 redshifts, 5299 star formation histories, and 4381 equivalent widths. Finally, a calculation of local density is presented and implemented in the VO catalogs for 66 164 galaxies. The latter is presented here for the first time.

Key words. catalogs – surveys – virtual observatory tools – galaxies: clusters: general – galaxies: fundamental parameters – galaxies: photometry

1. Introduction

The WIde-field Nearby Galaxy-cluster Survey (WINGS, Fasano et al. 2006) project was conceived to give a full description of galaxies in nearby clusters, and to provide a robust and homogeneous observational dataset to be used in the interpretation of galaxies in clusters at higher redshift.

In this context, current knowledge of the systematic properties of galaxies in nearby clusters remains surprisingly limited, being largely based on just the Virgo, Coma, Fornax clusters, and the Shapley supercluster (e.g., Gavazzi et al. 2003; Merluzzi et al. 2010). At higher redshifts, the LoCUSS survey has targeted galaxy clusters at $z \sim 0.2$, the STAGES project has studied in detail the A901/2 system at $z = 0.165$ (Smith et al. 2010; Gray et al. 2009), and a large amount of high quality data for more distant clusters is continuously being gathered with the *Hubble* Space Telescope (HST) and large ground-based telescopes.

Nevertheless, the morphological reference for local clusters is still provided by the historical database of Dressler (1980) based on photographic plates, giving the positions, the estimated magnitudes (down to $V \sim 16$), and the visual morphological classification for galaxies in 55 clusters in the range $0.011 \leq z \leq 0.066$. This awkward situation can be easily understood since a significant number of low redshift clusters could be mapped reasonably well only with the new large format (wide field) CCD mosaic cameras. On the other hand, morphological classifications are presently available for a large number of galaxies from the Sloan Digital Sky Survey (SDSS), which is not designed to be a cluster survey. In fact, morphological classifications are available only for the brightest sources ($g \leq 16$

Table 1. WINGS database in a nutshell.

Table name	Ref	Content	n(obj)	References
OPT	Sect. 3	Optical V (B) photometry	759 024	(1)
GASPHOTV	Sect. 3	Optical V surface brightness analysis	42 275	(2), (3)
GASPHOTB	Sect. 3	Optical B surface brightness analysis	41 463	(2), (3)
NIRK	Sect. 4	Near-infrared (K) photometry	962 344	(4)
NIRKJ	Sect. 4	Near-infrared (J) photometry	628 813	(4)
GASPHOTK	Sect. 4	Near-infrared (K) surface brightness analysis	71 687	(2), (3)
MORPHOT	Sect. 5	Morphology	39 923	(5)
REDSHIFT	Sect. 6.1	Redshift and membership	6132	(6)
SFHIST	Sect. 6.2	Star formation histories	5299	(7), (8)
EQWIDTH	Sect. 6.3	Equivalent widths	4381	(9)
LOCDENS	Sect. 7	Local densities	66 164	–

Notes. For each dataset we list in this table the section of the present paper where the dataset is described, the content of the dataset, the number of objects constituting the dataset, and the original paper with the detailed analysis.

References. (1) Varela et al. (2009); (2) Pignatelli et al. (2006); (3) Bindoni et al., in prep.; (4) Valentinuzzi et al. (2009); (5) Fasano et al. (2012); (6) Cava et al. (2009); (7) Fritz et al. (2007); (8) Fritz et al. (2011); (9) Fritz et al. (2014).

in Nair & Abraham 2010; Fukugita et al. 2007 and $r \leq 17$ in Willett et al. 2013) and thus are much less accurate than those provided by a dedicated survey (see, for example, the EFIGI catalog by Baillard et al. 2011, with detailed morphology but magnitude limit at $g = 14$).

The WINGS collaboration has started to fill the observational gap between very nearby clusters and high-redshift clusters by observing in the optical bands (B and V) 76 clusters of galaxies that span the largest possible range of cluster characteristics, as given by their X-rays properties.

We selected the WINGS clusters from three X-ray flux-limited samples compiled from ROSAT All-Sky Survey data: the ROSAT Brightest Cluster Sample (BCS, Ebeling et al. 1998), and its extension (eBCS, Ebeling et al. 2000) in the northern hemisphere and the X-Ray brightest Abell-type cluster sample (XBACs, Ebeling et al. 1996) in the southern hemisphere. The original WINGS sample comprises all clusters from BCS, eBCS, and XBACs with a high Galactic latitude ($|b| \geq 20$ deg) in the redshift range $0.04 < z < 0.07$. The redshift cut and the Galactic latitude are thus the only selection criteria applied to the X-ray samples. We refer the reader to the original paper by Fasano et al. (2006) for a description of the cluster sample (i.e., X-ray luminosities, temperatures, masses, Bautz-Morgan class distribution, and so on).

The optical CCD imaging data obtained for this sample of local clusters of galaxies is called WINGS-OPT, and is the main foundation upon which the WINGS project is based. From this set of mosaic images it has been possible to construct a photometric catalog of sources suitable for spectroscopic follow-up (from now on called WINGS-SPE, see Cava et al. 2009 for a more detailed description). Unfortunately, our spectroscopic program suffered from bad weather conditions, so the final WINGS-SPE sample contains 48 (of the 76) clusters, 22 of which are in the southern sky and 26 in the northern sky.

For a subsample of clusters, photometric data in the J and K near-infrared wavebands were added to the main photometric sample, via a dedicated program undertaken with the United Kingdom Infrared Telescope (UKIRT). Wide-field camera (WFCAM) observations were taken of 28 clusters (Valentinuzzi et al. 2009), making WINGS-NIR the largest near-infrared survey of nearby galaxy clusters in terms of area coverage. In fact, in this redshift range, only individual clusters or small cluster samples have been studied in the literature until now (e.g., Pahre 1999; Gavazzi et al. 1990; De Propris et al. 2003).

Dedicated observations with the INT, BOK, and LBT telescopes have also provided U band photometry for a subsample of 17 clusters (see Omizzolo et al. 2014).

Finally, the project is being expanded by very wide field observations (four times the original WINGS area) taken with Omegacam/VST in the usual B and V Johnson bands (Gullieuszik et al., in prep.) and in the Sloan u band. A program of follow-up spectroscopy using AAOmega/AAT is currently in progress, and we plan to release a second version of the database covering this larger area. The Omegacam/AAOmega dataset will extend out to between two and five times the projected virial radius of each cluster[1].

2. Overview of the database

To fully exploit the capabilities of the entire dataset, we decided to develop a local database of measurements, whose structure and size grows as the observations improve. The goal of the present paper is to describe the whole WINGS dataset, as available for download and use through Virtual Observatory (VO) tools. We decided to use this method to make the data public, since it is becoming more and more popular, and it is relatively easy to maintain a VO mirror of our local MySQL database.

Thus far, WINGS data have been published along with the paper describing them, through the Strasbourg astronomical Data Center (Centre de Données astronomiques de Strasbourg, CDS) (Varela et al. 2009; Cava et al. 2009; Valentinuzzi et al. 2009; Fritz et al. 2011; Bindoni et al., in prep.). However, these catalogs cannot be regularly updated. We, therefore, decided to make our data available using the VO, which allows for a more flexible treatment (and usage) of the data itself. The registration of WINGS services to the VO repository is maintained by the IA2 team in Trieste (Molinaro et al. 2012).

The structure of the database is very simple, as it has one unique primary key, which is the WINGS ID. Each new measurement (photometry, spectra, profiles, and so on) is then uploaded into the database with its own unique ID. The WINGS ID is a string field of 25 characters, which contains the coordinates of the object (right ascension and declination in hhmmss

[1] In all WINGS papers the virial radius of each cluster is taken to be equal to R_{200}, the radius delimiting a sphere with interior mean density 200 times the critical density, and is derived from the cluster velocity dispersion as in Cava et al. (2009).

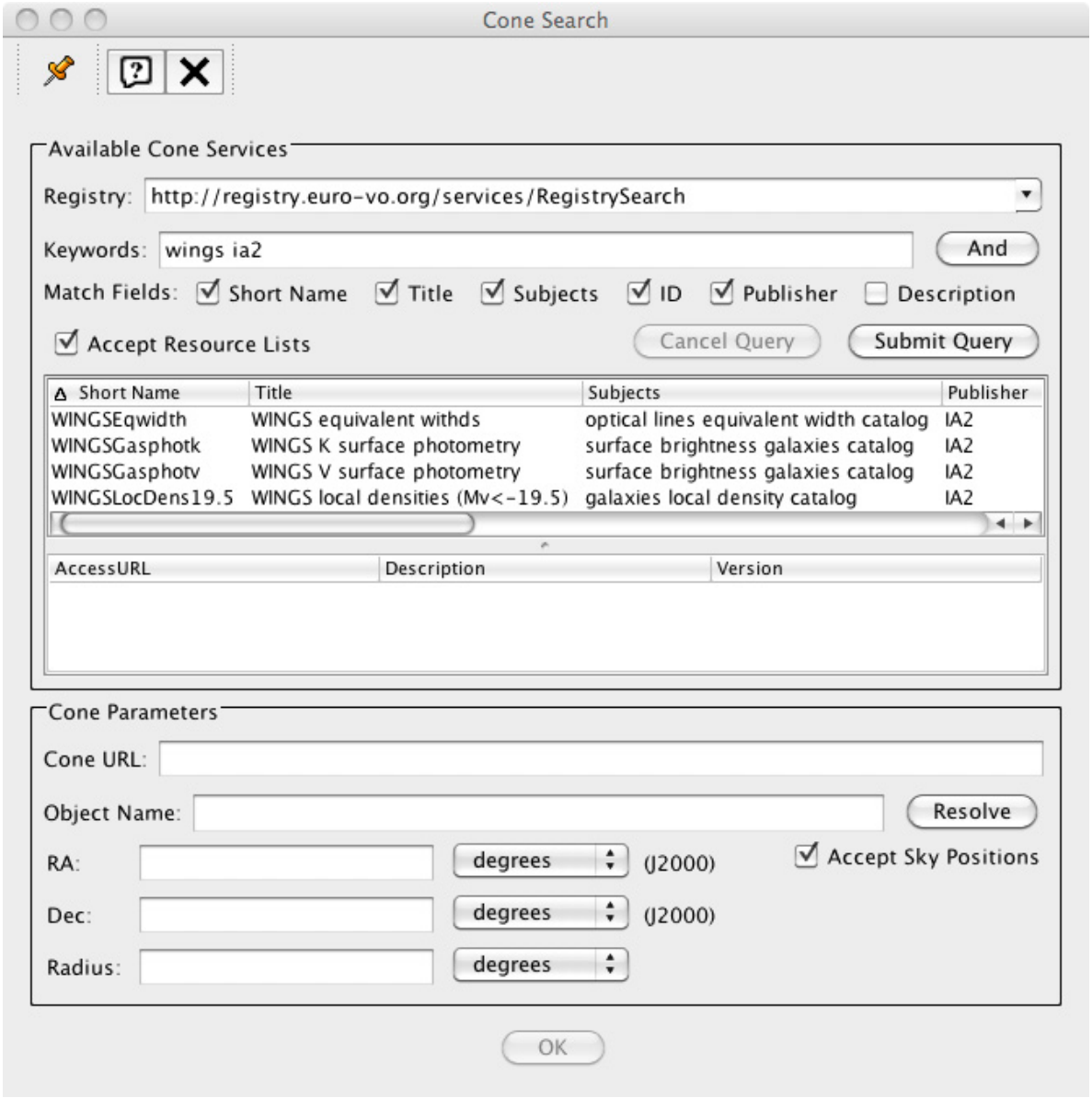

Fig. 1. A TOPCAT screenshot of the cone search query in the VO using the *wings ia2* keywords.

and deg). In order to avoid identifications that are not meaningful, each time a new measurement is made an appropriate series of routine checks are made for possible cross-matching objects inside a given coordinates box, whose size depends on the positioning error (due, for example, to the astrometry). We provide a summary of the different datasets presently constituting the WINGS archive, which are described in this paper, in Table 1. The number in the fourth column gives the total number of objects for each dataset.

Each one of the WINGS tables described in the present paper is available to the community as a cone search in the VO framework (Williams et al. 2011). We recommend looking at the VO registry[2], where the available dataset can be found by using the keyword WINGS. Those whose field *Publisher* is IA2 are described in this paper and updated in real time when needed. As a future development we will make the entire relational database available as a TAP service (Dowler et al. 2011) to allow for more complex queries. Figure 1 shows how to access WINGS data using the TOPCAT interface and the described keywords.

3. Optical catalogs: photometry and structural parameters [WINGS-OPT]

The core of the WINGS project is the optical photometry based on wide-field images of galaxy clusters at low redshift. The wide-field images were taken using the wide field cameras on either the 2.5 m *Isaac Newton* Telescope (INT/WFC) or the MPG/ESO-2.2 m telescope (ESO/WFI). The typical full width at half maximum (FWHM) for the whole set of six observing runs (three for each telescope) was ∼1.1 arcsec, while the magnitude limit was $M_V \sim -14$. The mosaic images, whose dimensions are $\sim 35' \times \sim 35'$, are available as Simple Image Access Protocol (SIAP) (Tody et al. 2011) through the VO tools (see Fig. 2 for an example). The IVOA identifier is `ivo://ia2.inaf.it/hosted/wings//opt`. The pixel scale is 0.333 arcsec/pix for the INT images, and 0.238 arcsec/pix for the WFI images. The WINGS photometry measurements were made from these

[2] http://registry.euro-vo.org/services/RegistrySearch

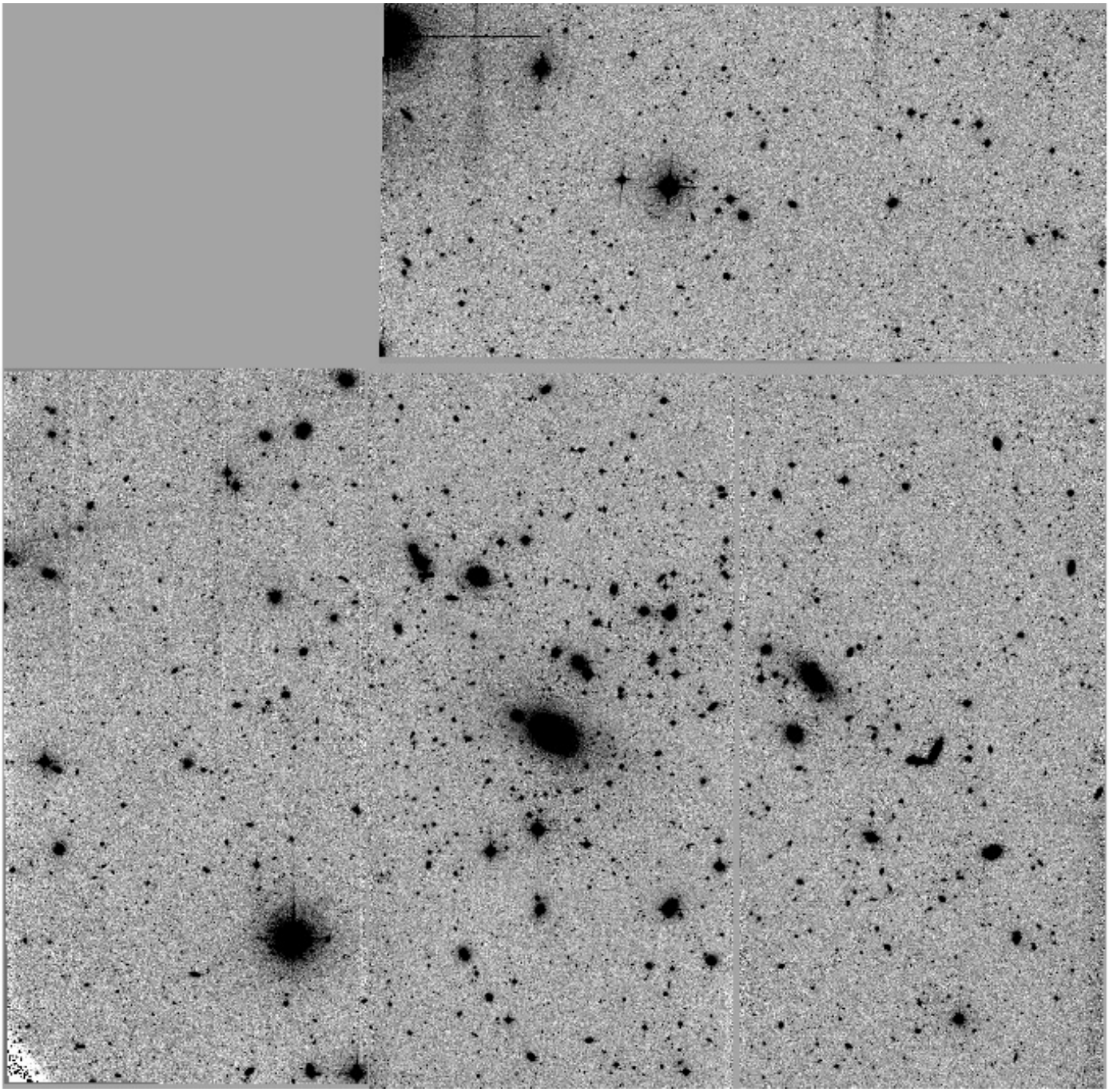

Fig. 2. INT image of the cluster A85 in the V band as it is available for download as SIAP from the VO.

images. These are described in Varela et al. (2009), and we also refer the reader to this paper for an assessment of the image quality. The mosaic construction is also described in Fasano et al. (2006). The header of each downloadable image also contains the photometric zeropoint.

Photometry was performed on the V-band images using Sextractor (Bertin & Arnouts 1996). The V-band image was used as a reference for the subsequent B-band photometry (run in single and in double image mode). At the end of the process, we kept only objects detected in both bands. We detected a total of 759 024 objects in 76 clusters, of which 394 280 are classified as galaxies in the V-band, 183 792 as stars, and the remaining as unknown. The WINGS classification (see Table 2) was mainly based on the Sextractor stellarity index and, as a starting point, we chose rather conservative limits: objects with a stellarity index smaller than 0.2 were initially flagged as galaxies, those with stellarity larger than 0.8 as stars, and objects in between as unknown. The final classification, however, took other diagnostics into account, and we refer the reader to the original paper (Varela et al. 2009) for a comprehensive description. Unknown objects start to contaminate the galaxy sample starting from $V = 21$, while at brighter magnitudes the fraction of misclassifications is negligible. At $V = 22.5$, the fraction of unknown objects rises to ∼20%, becoming similar to the fraction of stars. A statistical study, however, demonstrates that the star/galaxy classification holds up well to $V \sim 24$ (see Figs. 7 and 8 in Varela et al. 2009). The published table contains: the WINGS unique ID, as well as its sky coordinates and the cluster name; the classification (1 for galaxies, 2 for stars and 0 for unknown objects); the Sextractor internal binary flag, which is

Table 2. OPT table content.

Content	Units	Description
ID	–	WINGS identifier (unique)
RA	deg	Right ascension (J2000)
Dec	deg	Declination (J2000)
CLUSTER	–	Cluster name
CLASS	–	WINGS classification (1, 2 or 0)
SEX FLAG	–	Sextractor binary flag
AREA	arcsec^2	Isophotal area above analysis threshold
ELL	–	Ellipticity ($1 - b/a$)
THETA	deg	Sextractor position angle (CCW/x)
PA	deg	Position angle (N/E)
MU MAX	mag/arcsec^2	Peak surface brightness above background
V AUTO	mag	Kron-like elliptical aperture magnitude
V 2KPC	mag	Aperture mag, R = 2.15 kpc
V 5KPC	mag	Aperture mag, R = 5.38 kpc
V 10KPC	mag	Aperture mag, R = 10.77 kpc
V 160	mag	Aperture mag, D = 1.60 arcsec
V 200	mag	Aperture mag, D = 2.00 arcsec
V 216	mag	Aperture mag, D = 2.16 arcsec
V AUTO ERR	mag	Error on V mag from Varela et al. (2009)
B AUTO	mag	Kron-like elliptical aperture magnitude
B 2KPC	mag	Aperture mag, R = 2.15 kpc
B 5KPC	mag	Aperture mag, R = 5.38 kpc
B 10KPC	mag	Aperture mag, R = 10.77 kpc
B 160	mag	Aperture mag, D = 1.60 arcsec
B 200	mag	Aperture mag, D = 2.00 arcsec
B 216	mag	Aperture mag, D = 2.16 arcsec
B AUTO ERR	mag	Error on B mag from Varela et al. (2009)
BV 2KPC	mag	Aperture color $B - V$, R = 2.15 kpc
BV 5KPC	mag	Aperture color $B - V$, R = 5.38 kpc
BV 10KPC	mag	Aperture color $B - V$, R = 10.77 kpc
$D_{\rm OPT}$	arcsec	Distance from the cluster optical center
$D_{\rm XCEN}$	arcsec	Distance from the cluster X-ray center
$D_{\rm BCG}$	arcsec	Distance from the cluster BCG

Table 3. GASPHOT table content.

Content	Units	Description
ID	–	WINGS identifier (unique)
RA	deg	Right ascension (J2000)
Dec	deg	Declination (J2000)
CLUSTER	–	Cluster name
MAG GAS	mag	magnitude
MAG GAS ERR	mag	Error on the magnitude
$R_{\rm e}$	arcsec	Effective radius (along semi-major axis)
$R_{\rm e}$ ERR	arcsec	Error on the $R_{\rm e}$
$\langle\mu_{\rm e}\rangle$	mag/arcsec^2	Mean surface brightness
N	–	Sersic index
N ERR	–	Error on the Sersic index
AXRAT	–	Axial ratio
AXRAT ERR	–	Error on the axial ratio
FLAG	–	Quality flag

Notes. The same structure is present for the V, B, and K measurements.

useful to assess the photometric quality of the detected object at a glance (i.e., if it has close neighbors, if it is blended, and so on); the isophotal area above the analysis threshold; the ellipticity; the position angle both from Sextractor and the one given N/E; and the peak surface brightness above the background. Magnitudes given in the database were estimated at various physical apertures, namely 2.15 kpc, 5.38 kpc, 10.77 kpc at the cluster redshift, calculated using a standard cosmology of ($\Omega_{\rm M} = 0.3$, $\Omega_\Lambda = 0.7$, and $H_0 = 70$ km s^{-1} Mpc^{-1}). We also give aperture magnitudes for three fixed angular apertures of 1.6, 2.0, and 2.16 arcsec, corresponding to the fibre diameters of our spectroscopic observations. All magnitudes were calibrated taking the color equation into account, and were corrected for atmospheric absorption. Errors in the given magnitudes were calculated using the average relation shown in Fig. 3 of Varela et al. (2009). We also list three aperture colors, derived from the set of three aperture magnitudes. Finally, we give the distances of the given object from the optical center of its host cluster, the distance from the X-ray center and the distance from the BCG, all in arcsec. The maximum error is 0.08 mag in the V-band for sources brighter than $V = 20.5$ and 0.1 mag in the B-band down to $B = 21$. As an indicator of the color gradient, we also quote the $(B - V)$ color at 5 kpc (see Sect. 6.2 for further details).

We also ran the GASPHOT tool (Pignatelli et al. 2006) on the same mosaic images used to perform the photometry to analyze the surface photometry of WINGS galaxies and to derive their structural parameters. We derived such measurements for 42 278 galaxies in the V-band and for 41 463 galaxies in the B-band. The complete procedure, as well as an assessment of the performance of GASPHOT will be described in Bindoni et al., in prep. In brief, the tool is designed to run in a completely automatic mode and basically fits a single Sersic law, simultaneously, to the light profiles along the major and the minor axis of each galaxy, appropriately convolved with a position varying point spread function. The software performs a fit of the growth profiles, so that the weight is higher where the uncertainties are smaller (i.e., in the galaxy external regions), and it is lower in the cores, where the galaxy photometry might be affected by peculiarities such as point-like sources, dust lanes, bars, pseudo-bulges and so on. The GASPHOT tool measures the V magnitude, the effective radius, the mean surface brightness, the Sersic index, and the axial ratio for each galaxy, as listed in Table 3. The errors on the derived quantities estimated for 90% of the global sample are <0.1 mag for the V magnitude, <0.2 arcsec for the effective radius, <0.8 for the Sersic index, and <0.015 for the axial ratio.

Since each mosaic image has its own photometric quality, we flagged as bad measurements those that have errors in the derived parameters larger than the 98th percentile of the measurement errors in each cluster. Furthermore, we also flagged as bad those fits that show Sersic indices at the limits of the space parameters (i.e., $n_V = 0.5$ or $n_V = 8$). The quality flag is thus a binary number of eight digits converted into decimals. The first two digits are always zero, the remaining six are set to one when the solution is extreme (i.e., Sersic index =0.5 or =8) [3rd digit], and when the errors in the estimated parameters (magnitude [4th], effective radius [5th], Sersic index [6th], background [7th] and axial ratio [8th]) exceed the 98th percentile of the error distributions for the given cluster and filter. Therefore, the flag is 0 for good fits, 32 for fits that find extreme solutions (i.e. Sersic index =0.5 or 8), 2 for fits with too large error on the background estimation, and 16 for fits with too large error on the estimated magnitude. The binary flag was calculated in this way to recognize fits that are relatively bad, while we suggest using the absolute errors to check for absolute deviant fits.

4. Near-infrared catalogs: photometry and structural parameters [WINGS-NIR]

In order to better characterize WINGS cluster galaxies, in particular their stellar masses, without being biased by the latest star formation episode dominating the galaxy light in the

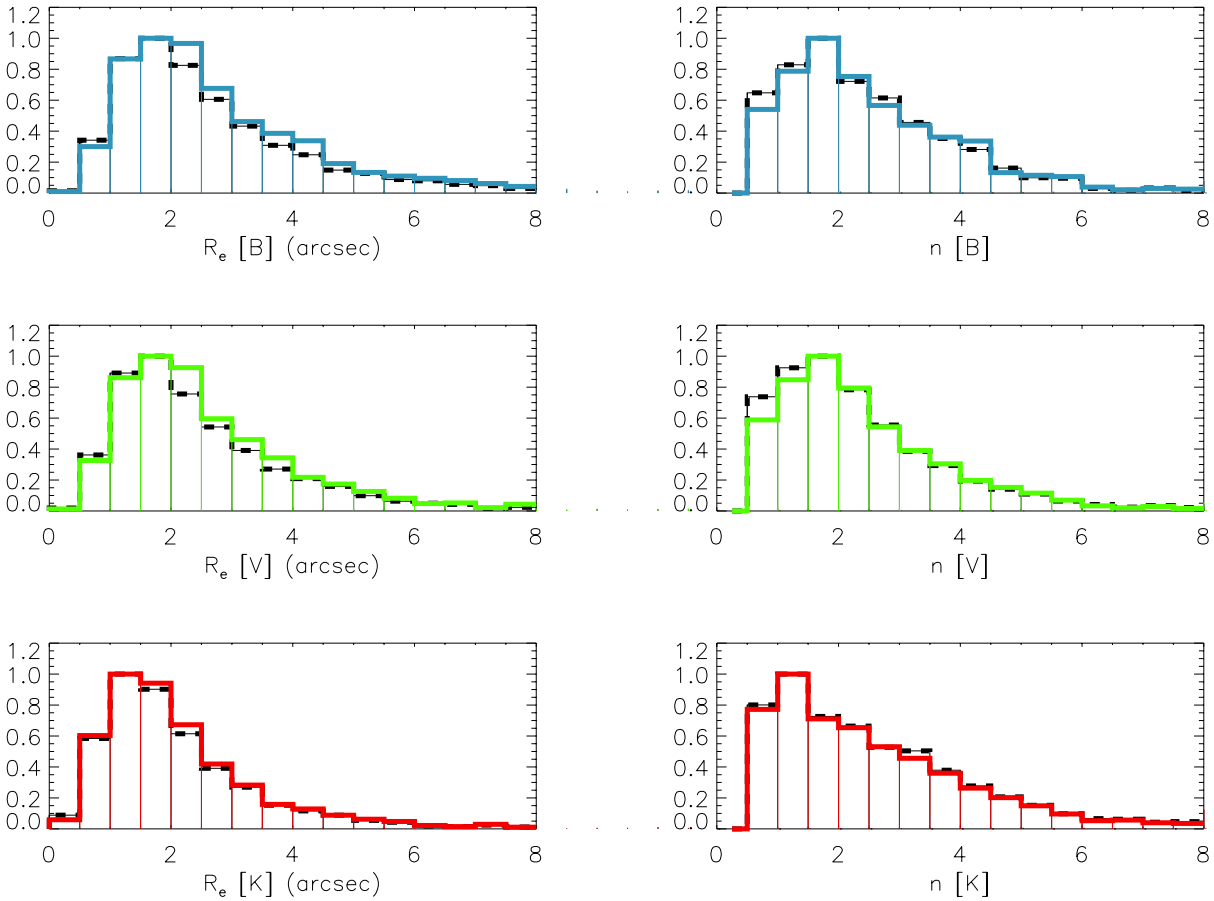

Fig. 3. Distribution of Sersic index (*right panels*) and effective radius (*left panels*) retrieved by GASPHOT for the spectroscopic members of our WINGS clusters in the three bands covered by our photometry: from top to bottom data are from the *B* images, the *V* images, and the *K* images. Dashed black lines refer to the entire WINGS sample, while the colored continuous lines are for the spectroscopic members observed in the three bands.

visible bands, WINGS is complemented by ancillary observations in the infrared bands taken with UKIRT/WFCAM. A complete description of the data reduction and quality assessment can be found in Valentinuzzi et al. (2009). We obtained observations in several runs (∼14) with a median seeing of ∼1.0 arcsec, and the final photometric catalogs have a 90% completeness of 19.4, 20.5 in the *K* and *J* band, respectively. Only a subsample of 28 clusters (17 clusters were observed in both bands) have the needed photometric accuracy. These, however, cover the entire range of X-ray luminosities of our original sample of clusters. The redshift distribution is representative of the entire sample as well, while the sample is slightly biased toward the low velocity dispersion tail of the cluster distribution. The WFCAM data reduction and photometric calibration was performed by the Cambridge Astronomical Survey Unit (CASU) team (Irwin et al. 2004; Hodgkin et al. 2009). The area covered by observations corresponded to ∼0.79 deg^2 for each cluster, thus making WINGS-NIR by far the largest survey of nearby galaxy clusters as far as the area coverage is concerned. In fact, in this redshift range, only individual clusters or small cluster samples have been studied in the literature up until now (e.g., Pahre 1999; Gavazzi et al. 1990; De Propris et al. 2003). The WINGS survey of near-infrared data consists of 962 344 (628 813) sources in *K* (*J*) bands, of which 490 034 (263 116) are galaxies. The star/galaxy classification was based again on the Sextractor stellarity parameters, but we used a value of 0.35 (instead of 0.2, see Sect. 3) to tag galaxies. We chose these parameters on the basis of the results of our artificial star tests. This initial classification was then refined by using interactive cleaning of different populations in appropriate diagnostic plots. We refer the reader to the original paper by Valentinuzzi et al. (2009) for further details. The structure of the NIRK and NIRJ tables of the WINGS database is analogous to that of the OPT table, and is shown in Table 4. The VO table contains the unique WINGS ID, its sky coordinates, the cluster name, the WINGS classification, the WINGS binary flag (described below), the area, ellipticity and position angle (CCW/x), the peak surface brightness above the background, the Sextractor AUTO magnitude, as well as the aperture magnitudes inside 2.15, 5.38, 10.77 kpc and inside 1.60, 2.00, 2.16 arcsec. The errors on magnitudes are calculated following Eq. (7) in Valentinuzzi et al. (2009). Finally, we list for each object its distance in arcsec from the optical and X-ray centers and from the BCG. The maximum error is 0.06 mag in both infrared bands for sources brighter than 16.5.

The WINGS flag is calculated as follows:

$$\text{WINGS FLAG} = a_1 + 2a_2 + 4a_3 + 8a_4 \quad (1)$$

where

- $a_1 = 1$ if classified as galaxy;
- $a_2 = 1$ if classified as star;
- $a_1 = a_2 = 0$ if classified as unknown;
- $a_3 = 1$ if weakly affected by neighboring halo; and

Table 4. NIRK-NIRJ table content.

Content	Units	Description
ID	–	WINGS identifier (unique)
RA	deg	Right ascension (J2000)
Dec	deg	Declination (J2000)
CLUSTER	–	Cluster name
CLASS	–	WINGS classification (1, 2 or 0)
WINGS FLAG	–	WINGS binary flag
AREA	arcsec^2	Isophotal area above analysis threshold
ELL	–	Ellipticity ($1 - b/a$)
THETA	deg	Sextractor position angle (CCW/x)
MU MAX	mag/arcsec^2	Peak surface brightness above background
K, J AUTO	mag	Kron-like elliptical aperture magnitude
K, J 2KPC	mag	Aperture mag, $R = 2.15$ kpc
K, J 5KPC	mag	Aperture mag, $R = 5.38$ kpc
K, J 10KPC	mag	Aperture mag, $R = 10.77$ kpc
K, J 160	mag	Aperture mag, $D = 1.60$ arcsec
K, J 200	mag	Aperture mag, $D = 2.00$ arcsec
K, J 216	mag	Aperture mag, $D = 2.16$ arcsec
K, J AUTO ERR	mag	Error on K, J mag from Valentinuzzi et al. (2009)
$D_{\rm OPT}$	arcsec	Distance from the cluster optical center
$D_{\rm XCEN}$	arcsec	Distance from the cluster X-ray center
$D_{\rm BCG}$	arcsec	Distance from the cluster BCG

Table 5. MORPHOT table content.

Content	Units	Description
ID	–	WINGS identifier (unique)
RA	deg	Right ascension (J2000)
Dec	deg	Declination (J2000)
CLUSTER	–	Cluster name
$T_{\rm ML}$	–	Morphology from Max. likelihood technique
$T_{\rm ML}^{\rm min}$	–	Lower limit of $T_{\rm ML}$
$T_{\rm ML}^{\rm max}$	–	Upper limit of $T_{\rm ML}$
$T_{\rm NN}$	–	Morphology from Neural Network technique
$T_{\rm NN}^{\rm min}$	–	Lower limit of $T_{\rm NN}$
$T_{\rm NN}^{\rm max}$	–	Upper limit of $T_{\rm NN}$
$T_{\rm M}$	–	Morphology from both techniques
$T_{\rm M}^{\rm min}$	–	Lower limit of $T_{\rm M}$
$T_{\rm M}^{\rm max}$	–	Upper limit of $T_{\rm M}$
$T_{\rm VIS}$	–	Visual type (if any)
TYPE	–	Final MORPHOT type

– $a_4 = 1$ if strongly affected by neighboring halo.

We ran the GASPHOT code to determine the structural parameters of our sample of galaxies on the same K band images used to perform the photometric analysis. This provided information for 71 687 galaxies. The corresponding table (called *gasphotk*) contains the same quantities described in Table 3. For a subsample of 1254 galaxies, which are spectroscopic members of the WINGS clusters, we have the structural parameters in the three bands (B, V, K). This subsample is limited by the spectroscopic incompleteness (about 50% of the observed targets turned out to be cluster members) and by the fact that not all clusters were actually observed in the K band. Figure 3 shows the distribution of the Sersic index (right panel) and the effective radius circularized (left panel) for these galaxies as continuous lines (while the dashed lines in black correspond to the entire population, normalized to the same peak value). As shown in the histograms of the effective radius, the light in K band is much more concentrated than in the visible bands, i.e., the mass (mainly traced by the infrared bands) is more concentrated than the light emitted in the visible bands, as expected. This obviously also reflects in the Sersic index distributions. The properties of member galaxies do not seem too much different from the overall distribution. The scientific interpretation of these distributions is going to be presented in a forthcoming paper.

5. Morphology

The morphological classification of cluster galaxies is one of the most important goals of the WINGS survey. Although visual classifications are generally believed to be more reliable than any automatic classification method, the advent of large mosaic CCDs has posed a big challenge to galaxy classifiers, since it is impractical to visually classify the tens of thousands galaxies imaged in large surveys.

A remarkable effort to acquire visual classifications of huge galaxy samples was performed by the Galaxy Zoo team (Lintott et al. 2008, 2011), which recently made available the visual classifications for about 900 000 galaxies from the Sloan Digital Sky Survey, as derived from the contribution of more than 100 000 volunteers. However, the voluntary-based nature of these classifications makes them necessarily coarse and only capable of distinguishing between elliptical and spiral galaxies.

Many different approaches to automatic classification have been proposed in the literature. Some of them have been widely used, as large amounts of high quality data have become available. Most automatic classifiers are based on morphological proxies, such as concentration, asymmetry, clumpiness, M20, the Gini coefficient, etc. (see Abraham et al. 1996, 2003; Conselice 2003; Lotz et al. 2004; Lauger et al. 2005; Scarlata et al. 2007; van der Wel 2008; Shamir 2009; Cheng et al. 2011, among the others).

The MORPHOT tool (Fasano et al. 2012) combines a large set (21) of diagnostics, easily computable from the digital cutouts of galaxies, producing two different estimates of the morphological type based on: (i) a semi-analytical maximum likelihood technique; (ii) a neural network machine. The final estimator has been tested over a sample of 1000 visually classified WINGS galaxies, proving to be almost as effective as the "eyeball" estimates themselves. In particular, at variance with most existing tools for automatic morphological classification of galaxies, MORPHOT has been shown to be capable of distinguishing between ellipticals and S0 galaxies with unprecedented accuracy.

The WINGS-MORPHOT catalog contains the morphological classifications of 39 923 galaxies, 2963 of which have also been classified visually. The numerical code adopted for morphology closely follows the revised Hubble type classification, apart from cD galaxies being given a tag of −6 by MORPHOT, instead of −4. The final morphological type given in the catalog is that from the visual classification if available, while in all other cases it is the mean of the two estimates provided by the maximum-likelihood (ML) and neural network (NN) techniques (see Fasano et al. 2012, for further details).

For each entry in the MORPHOT table, besides the unique WINGS ID, we give (see Table 5) the sky coordinates, the cluster name, the morphological types derived from the ML and NN techniques, along with the relative confidence intervals, the mean morphological type (again with the proper confidence interval), the visual type (when available), and the final type that we propose to the astronomical community for any scientific use. Details about the computation of the confidence intervals are given in Appendix B of Fasano et al. (2012).

6. Spectroscopic sample [WINGS-SPE]

Another primary goal of the WINGS survey is to produce a large dataset of galaxies in clusters with good quality spectra. Because of the large field of view of the photometric sample, it has been possible to define candidates for the spectroscopic follow up out to large distances from the cluster center (usually up to $\sim 0.5 \times R_{\rm vir}$, but up to $R_{\rm vir}$ in some cases). The target selection takes advantage of the WINGS photometric catalog (Varela et al. 2009), already described in Sect. 3. To maximize the probability of observing galaxies at the cluster redshift without biasing the cluster sample, targets were selected on the basis of their properties so that background galaxies (redder than the cluster red sequence) could be reasonably avoided. In particular, the spectroscopic sample included only those galaxies with $V \leq 20$ (total magnitude), $V_{\rm fiber} < 21.5$, and $(B-V)_{5\ {\rm kpc}} \leq 1.4$. This last cut was slightly varied from cluster to cluster to optimize the observational setup. The number of targets with $V \leq 20$ is 30 126 in the global photometric sample, and 19 244 in the 48 clusters which were followed up spectroscopically. This reduces to 28 861 (and 18 476, respectively) after having imposed the fiber magnitude cut.

Our total apparent magnitude limit ($V \sim 20$) is 1.5 to 2.0 mag deeper than the 2dFRS and Sloan surveys, and this is, in general, reflected in a higher mean number of member galaxies detected per cluster. We performed our spectroscopic observations over the course of six observing runs (22 nights) at the 4.2 m *William Herschel* Telescope (WHT), using the AF2/WYFFOS multifiber spectrograph, and three observing runs (11 nights) at the 3.9 m Anglo Australian Telescope (AAT), using the 2dF multifiber spectrograph.

In both cases, the spectral range covers the optical range (~3800–7000 Å and ~3600–8000 Å) where the most commonly used diagnostic lines are located (from the Ca H&K in the blue to NaD in the red). The dispersion was ~6 Å and ~9 Å, while the nominal fiber aperture was 1.6″ and 2″, respectively. Spectra for galaxies in only 48 of the original 76 clusters were obtained, because of bad weather conditions during the course of the observations, especially in the case of the northern sample.

6.1. Redshift and membership

We measured redshifts from the spectra using a semi-automatic method, which involves the automatic cross-correlation technique (as implemented in the *xcsao* IRAF task) and the emission lines identification.

We used an iterative $\pm 3\sigma$ clipping method (Beers et al. 1990) to determine which galaxies were cluster members and this resulted in an estimate of the cluster velocity dispersion with an average number of galaxies that was up to three times larger than that used in previous studies of the same clusters. The spectroscopic completeness of the sample varies among the two datasets, being higher for the southern sample, where we have a spectroscopic completeness of 50% at $V = 19.5$ and could measure redshifts for 75% of the galaxies. For the northern sample, the situation is worse because of bad weather conditions during the observing runs (see Cava et al. 2009, for details).

The WINGS redshift table contains redshifts and memberships for 6132 galaxies, 3694 of which are tagged as cluster members. Table 6 shows the catalog entries. The coordinates are those centered on the fiber, while errors on the redshift measurements are correlated with the amplitude of the correlation peak, as described in Cava et al. (2009) and references therein. The typical error is ~25 km s^{-1}. The membership is set to 1 if the galaxy is considered to be a cluster member, otherwise it is set to 0.

Table 6. REDSHIFT table content.

Content	Units	Description
ID	–	WINGS identifier (unique)
RA	deg	Right ascension (J2000)
Dec	deg	Declination (J2000)
cz	km s^{-1}	Heliocentric velocity
Err(cz)	km s^{-1}	Heliocentric velocity error
z	–	Redshift
membership	–	Membership

6.2. Star formation histories

For the subsample of 5299 galaxies with the highest signal-to-noise ratio (~15) spectra, we also derived star formation histories via spectro-photometric modeling (Fritz et al. 2011). In brief, we used a combination of single stellar population models (SSPs) of different ages to derive the galaxy star formation history using a minimization technique. The SSPs spanned a range of ages between 10^6 and 14.1×10^9 years and were calculated for three different metallicities (i.e. $Z/H = 0.004$, 0.02 and 0.05). For each metallicity value, many realizations of the galaxy star formation history (SFH) were calculated, with the final result coming from the realization that minimized the difference between the observed and calculated quantities. In practice, the χ^2 value was calculated as the weighted difference between the calculated and observed continuum fluxes and equivalent widths of the visible lines (both absorption and emission). The amount of dust was also a free parameter of the model, which varied with the age of the SSP.

This approach does not take the chemical evolution of the galaxy into account, as it implicitly assumes that the overall population of the galaxy has just one, single metallicity. However, Fritz et al. (2007, 2011) demonstrated that this assumption does not significantly bias the stellar mass determination. The adopted SSPs were those calculated using the isochrones of Bertelli et al. (1994) and a standard Salpeter IMF over the mass range 0.15–120 $M_\odot$.

We used the model also to compute galaxy stellar masses, based on the fiber aperture and total magnitudes (assuming no color gradient in the region between the fiber and the total extent of the galaxy), metallicity (intended as the metallicity of the best fit model), ages (both luminosity and mass weighted), average star formation rates in four main bins of age ($0–2 \times 10^7$, $2 \times 10^7–6 \times 10^8$, $6 \times 10^8–5.6 \times 10^9$ and $5.6 \times 10^9–14 \times 10^9$ years), as well as fiber and total (model) magnitudes in the whole range of observational filters (as detailed in the CDS version of the table).

The masses given in the table are of three types, as described in Fritz et al. (2007, 2011) and references therein. When transforming fiber masses to total masses the implicit assumption of no color gradient between the fiber aperture and the total galaxy magnitude is made. However, we also have at our disposal the color gradient, since we measured B and V magnitudes at different distances from the galaxy centers. Therefore, we also list in the final table a term called *ccol*, computed using the fiber color and the color measured at 5 kpc from the galaxy center, which should be added to the total masses to take the color gradients into account.

In Table 7 we list, for each of the 5299 galaxies, the metallicity of the best fit model; the young stars and total V-band

Table 7. SFHIST table content.

Content	Units	Description
ID	–	WINGS identifier (unique)
RA	deg	Right ascension (J2000)
Dec	deg	Declination (J2000)
metal	–	best metallicity value
A_V(young)	mag	V-band extinction of young stars
A_V(tot)	mag	Total V-band extinction
sfr1	$M_\odot$/yr	Star Formation Rate in the 0−2e7 yr range
sfr2	$M_\odot$/yr	Star Formation Rate in the 2e7−6e8 yr range
sfr3	$M_\odot$/yr	Star Formation Rate in the 6e8−5.6e9 yr range
sfr4	$M_\odot$/yr	Star Formation Rate in the 5.6e9−14.1e9 yr range
$m1_{\rm fib}$	$M_\odot$	Fiber Mass 1
$m2_{\rm fib}$	$M_\odot$	Fiber Mass 2
$m3_{\rm fib}$	$M_\odot$	Fiber Mass 3
$m1_{\rm tot}$	$M_\odot$	Total Mass 1
$m2_{\rm tot}$	$M_\odot$	Total Mass 2
$m3_{\rm tot}$	$M_\odot$	Total Mass 3
ccol	–	color term
LWAGE	yr	(Log10 of) Luminosity weighted age
MWAGE	yr	(Log10 of) Mass weighted age

extinction calculated from the model; the star formation rates in four (broad but significant) bins of age; the stellar masses (inside the fiber and total) as, (1) the mass of gas turned into stars; (2) the stellar mass, including mass locked up in remnants; and (3) the mass of stars still alive; the color term correction; and the galaxy ages (both the luminosity and mass weighted). The typical error on the masses is 0.2 dex, while the maximum error on the age determination is ∼1 Gyr (Fritz et al. 2011).

6.3. Equivalent widths

A second set of measurements concerns the estimation of line equivalent widths (EW), which have been demonstrated to be a powerful tool to estimate stellar population properties (ages, star formation histories, metallicities, and so on).

Line equivalent widths were measured in the WINGS spectra using an automated method described in detail in Fritz et al. (2014). Among the original spectroscopic sample consisting of ∼6000 galaxies, we discarded those having unrecoverable difficulties in the wavelength calibration shortward of ∼4300 Å. Moreover, we also eliminated from the final sample all galaxies belonging to clusters in which less than 20 objects turned out to be cluster members. At the end of the selection procedure, only seven clusters from the northern sample possessed spectra that are included in the final catalog of 4381 objects, the remainder coming from the southern sample.

The measured spectral lines are listed in Table 1 of Fritz et al. (2014) and are listed in the database columns that we make publicly available (see Table 8). Following the WINGS ID with its sky coordinates, we list equivalent widths of OII, H_θ, H_ζ, H_η, Ca(K), Ca(H)+H_ϵ, H_δ, Gband, H_γ, H_β, OIII, Mg, Na, H_α, D4000, D_n4000. We also give a classification (that is described below) and a completeness factor.

As for the completeness of the sample, we take both luminosity and geometrical completeness into account. The total weight for each analyzed galaxy in the sample is defined as:

$$W(m,r)_i = \frac{1}{(C(m)_i \times C(r)_i)} \quad (2)$$

where $C(m)_i$ and $C(r)_i$ are the magnitude and geometrical completeness in the bin to which the galaxy belongs.

Table 8. EQWIDTH table content.

Content	Units	Description
ID	–	WINGS identifier (unique)
RA	deg	Right ascension (J2000)
Dec	deg	Declination (J2000)
OII	Å	Equivalent width of OII [3727 Å]
Err(OII)	Å	Error on Equivalent width of OII [3727 Å]
H_θ	Å	Equivalent width of H_θ[3798 Å]
Err(H_θ)	Å	Error on Equivalent width of H_θ [3798 Å]
H_ζ	Å	Equivalent width of H_ζ[3889 Å]
Err(H_ζ)	Å	Error on Equivalent width of H_ζ [3889 Å]
H_η	Å	Equivalent width of H_η[3835 Å]
Err(H_η)	Å	Error on Equivalent width of H_η [3835 Å]
Ca(K)	Å	Equivalent width of Ca(K) [3934 Å]
Err(Ca(K))	Å	Error on Equivalent width of Ca(K) [3934 Å]
Ca(H)+H_ϵ	Å	Equivalent width of Ca(H)+H_ϵ [3969 Å]
Err(Ca(H)+H_ϵ)	Å	Error on Equivalent width of Ca(H)+H_ϵ [3969 Å]
H_δ	Å	Equivalent width of H_δ[4101 Å]
Err(H_δ)	Å	Error on Equivalent width of H_δ [4101 Å]
Gband	Å	Equivalent width of Gband [4305 Å]
Err(Gband)	Å	Error on Equivalent width of Gband [4305 Å]
H_γ	Å	Equivalent width of H_γ[4341 Å]
Err(H_γ)	Å	Error on Equivalent width of H_γ [4341 Å]
H_β	Å	Equivalent width of H_β[4861 Å]
Err(H_β)	Å	Error on Equivalent width of H_β [4861 Å]
OIII	Å	Equivalent width of OIII [5007 Å]
Err(OIII)	Å	Error on Equivalent width of OIII [5007 Å]
Mg	Å	Equivalent width of Mg [5177 Å]
Err(Mg)	Å	Error on Equivalent width of Mg [5177 Å]
Na	Å	Equivalent width of Na(D) [5890 + 5895 Å]
Err(Na)	Å	Error on Equivalent width of Na(D) [5890 + 5895 Å]
H_α	Å	Equivalent width of H_α[6563 Å]
Err(H_α)	Å	Error on Equivalent width of H_α [6563 Å]
D4000	Å	Equivalent width of D4000 index (def. Bruzual 1983)
D_n4000	Å	Equivalent width of D_n4000 index (def. Balogh 1999)
Class	–	Classification flag (see text)
MagWeight	–	Magnitude weight (see Eq. (3))
RadWeight	–	Geometrical weight (see Eq. (4))

The magnitude completeness accounts for the fact that not all the galaxies in each magnitude bin fulfill the selection criteria used for the spectroscopic sample. The completeness as a function of magnitude is therefore defined as:

$$C(m) = \frac{N_z}{N_{\rm ph}}(m) \quad (3)$$

where N_z is the number of galaxies with measured redshifts, and $N_{\rm ph}$ is the number of galaxies in the parent photometric catalog, taking the cuts in color and magnitude into account, for each given magnitude bin m.

Moreover, we also computed the radial completeness for the WINGS sample, because fiber collisions and superpositions are not allowed. However, we carried out WINGS observations with more than one configuration, with the result that the radial completeness function is close to being flat. In an analogous way to the magnitude completeness, the radial completeness is defined as:

$$C(r) = \frac{N_z}{N_{\rm ph}}(r) \quad (4)$$

where the bins are at varying radial distances from the center.

On the basis of these EW measurements (in particular, [OII] and H_δ), we also provide a spectral classification of our WINGS spectra, following the definitions given in Dressler et al. (1999). Broadly speaking, we classified as *e(a)*, *e(b)* and *e(c)* all emission line galaxies with supposedly high values of dust obscuration (value 1), and stronger or weaker emission (values 2 and 3 in the database catalog). Instead, passive galaxies are labeled as k, $k+a$, $a+k$, the latter two classes showing the signature

Table 9. LocDens table content.

Content	Units	Description
ID	–	WINGS identifier (unique)
RA	deg	Right ascension (J2000)
Dec	deg	Declination (J2000)
LD	N/Mpc^2	(Decimal) Log of the nr. of galaxies per Mpc^2
WLD	%area	Coverage field fraction
CCDX	R_{200}/pix	Distance from the Xray cluster center
WCCDX	%area	Coverage field fraction at CCDX
CCDB	R_{200}/pix	Distance from the BCG
WCCDB	%area	Coverage field fraction at CCDX

of recent, but currently absent star formation (values 4, 5, and 6 of the catalog). When the [OII] emission line was not detectable, we used H_β and [OIII] to distinguish emission line galaxies from passive galaxies. A more detailed and careful description of the classification procedure, as well as an accurate description of our error evaluation, is given in Fritz et al. (2014).

7. Local densities

The last piece of information added to the WINGS dataset is the local density of galaxies, which we calculated to evaluate whether or not galaxy properties in clusters depend on the local environment. Vulcani et al. (2012) already used this quantity to study the dependence of the galaxy mass function on the environment. Briefly, we recall here how the local density was computed, and the meaning of the published columns of Table 9. For each spectroscopically confirmed cluster member, we calculated the area of the circle containing its ten nearest projected neighbors with photometry available and whose absolute magnitudes are brighter than $M_V = -19.5$, assuming they are cluster members. Some of these galaxies will obviously be foreground or background field galaxies, and so these were subtracted statistically by using the counts given in Berta et al. (2006). A correction was also made to the local densities calculated for galaxies that lie at the edges of our WINGS images. In these cases, the area covered by the observations is smaller than the calculated area, their ratio being defined as the coverage factor. The correction was applied by multiplying the number counts by this coverage factor and then doing the field galaxy subtraction. In both cases the area A_{10} used was that obtained by interpolation between the two areas for which the corrected counts are immediately lower and higher than 10 (since the field number counts are not integer numbers in the canonical A_{10} definition). This computation was made for all WINGS galaxies brighter than $M_V = -16$. Note that for clusters lacking a velocity dispersion measurement (namely A311, A2665, A3164, and Z1261), the distances are given in pixels and not in terms of R_{200}. In Table 9, we list the data available in the VO, i.e., the local density of galaxies brighter than $M_v <= -19.5$ per Mpc^2 (LD), the percentage of area effectively covered by the observations (WLD), the distance from the X-ray center in units of R_{200} or pixels (CCDX), and the percentage of circular area covered by the mosaic (WCCDX). These last two quantities were calculated with respect to the BCG as well (CCDB and WCCDB, respectively).

8. Summary

The WINGS survey has obtained data for 76 nearby clusters of galaxies. Here we describe and present the entire ensemble of WINGS catalogs derived as part of this survey, where the access key is the WINGS ID.

In the near future, we plan to produce new spectroscopic and photometric datasets for the outer regions of our cluster sample. The data will be available through the VO tools and hosted at the Italian Center for Astronomical Archives (IA2).

The released database contains optical (B, V) photometry for 759 024 sources (of which 394 280 are classified as galaxies) in 76 clusters at redshift ∼0.01–0.07, with a maximum error of 0.08 mag in the V-band (to $V = 20.5$) and 0.1 mag in the B band (to $B = 21$). These data are supplemented by near-infrared (J and K) photometry for 628 813 (in J) and 962 344 (in K) sources in 17 clusters (11 clusters have only the K-band photometry) with an error of 0.06 mag up to $K, J = 16.5$.

We also provide measurements of the Sersic index, mean surface brightness, axial ratio, effective radius, and ellipticity for subsamples of 42 278 galaxies in the V-band, 41 463 galaxies in the B-Band, and 71 687 galaxies in the near-infrared bands. Morphological classification are also given for 39 923 galaxies. Finally, we measured redshifts for 6132 galaxies, of which 3694 are cluster members. Errors on the redshift measurements are typically 25 km s^{-1}.

Finally, two other catalogs are provided with information that complements the rest of the dataset: (i) a catalog containing star formation history information that includes masses, ages, and star formation rates for 5299 galaxies; (ii) a catalog giving equivalent width measurements for 4381 galaxies. The errors on the derived masses are of the order of 10% (median), and the maximum error on the ages is ∼1 Gyr. An estimate of the local galaxy density (for neighbors brighter than $M_V = -16$) has been calculated as well, taking the field coverage factors into account.

In order to download the data, the user needs to access the VO-registry and use the keyword WINGS. Two types of data can be searched for: the wide-field images as a SIAP protocol, and scientific catalogs as a cone search. If accessing the VO with TOPCAT (Taylor 2005), these two choices are listed under the VO tab. To access the data, the user must first select the appropriate registry[3] and then insert the keywords WINGS and ia2 (to avoid other catalogs with different publishers). Once the resource has been selected, i.e., after clicking on the line with the chosen source, other parameters become available, i.e., one can look for a particular object name, or a particular position in the sky. In both cases, the physical dimension of the search box must be specified. The typical screenshot is shown in Fig. 1. The results of these queries are a list of images that can be seen using related VO software (such as *Aladin*), for the SIAP, and the catalog table for the cone search. Crossmatches between different tables/catalogs are possible, using the WINGS ID (i.e., the primary key of the database). The entire relational database will be made available to the community soon using the TAP service of the VO (Dowler et al. 2011), thus allowing the database to be queried using the ADQL language.

Future releases of the database will include photometry in the U- and u-bands (Omizzolo et al. 2014), B- and V-band photometry for the outer cluster regions (based on VST observations), and analysis of spectra taken of galaxies in the outer regions with the AAT/AAOmega spectrograph.

Acknowledgements. B.V. is supported by World Premier International Research Center Initiative (WPI), MEXT, Japan.

[3] http://registry.euro-vo.org/services/RegistrySearch

References

Abraham, R., Tanvir, N., Santiago, B., et al. 1996, MNRAS, 279
Abraham, R. G., van den Bergh, S., & Nair, P. 2003, ApJ, 588, 218
Baillard, A., Bertin, E., de Lapparent, V., et al. 2011, A&A, 532, A74
Beers, T. C., Flynn, K., & Gebhardt, K. 1990, AJ, 100, 32
Berta, S., Rubele, S., Franceschini, A., et al. 2006, A&A, 451, 881
Bertelli, G., Bressan, A., Chiosi, C., Fagotto, F., & Nasi, E. 1994, A&AS, 106
Bertin, E., & Arnouts, S. 1996, A&AS, 117, 393
Cava, A., Bettoni, D., Poggianti, B. M., et al. 2009, A&A, 495, 707
Cheng, J. Y., Faber, S. M., Simard, L., et al. 2011, MNRAS, 412
Conselice, C. J. 2003, ApJS, 147, 1
De Propris, R., Colless, M., Driver, S. P., et al. 2003, MNRAS, 342, 725
Dowler, P., Rixon, G., & Tody, D. 2011 [arXiv:1110.0497]
Dressler, A. 1980, ApJ, 236, 351
Dressler, A., Smail, I., Poggianti, B. M., et al. 1999, ApJS, 122, 51
Ebeling, H., Voges, W., Bohringer, H., et al. 1996, MNRAS, 281, 799
Ebeling, H., Edge, A. C., Bohringer, H., et al. 1998, MNRAS, 301, 881
Ebeling, H., Edge, A. C., Allen, S. W., et al. 2000, MNRAS, 318, 333
Fasano, G., Marmo, C., Varela, J., et al. 2006, A&A, 445, 805
Fasano, G., Vanzella, E., Dressler, A., et al. 2012, MNRAS, 420, 926
Fritz, J., Poggianti, B. M., Bettoni, D., et al. 2007, A&A, 470, 137
Fritz, J., Poggianti, B. M., Cava, A., et al. 2011, A&A, 526, A45
Fritz, J., Poggianti, B., Cava, A., et al. 2014, A&A, accepted [arXiv:1402.4131]
Fukugita, M., Nakamura, O., Okamura, S., et al. 2007, AJ, 134, 579
Gavazzi, G., Trinchieri, G., & Boselli, A. 1990, A&AS, 86, 109
Gavazzi, G., Boselli, A., Donati, A., Franzetti, P., & Scodeggio, M. 2003, A&A, 400, 451
Gray, M. E., Wolf, C., Barden, M., et al. 2009, MNRAS, 393, 1275
Hodgkin, S. T., Irwin, M. J., Hewett, P. C., & Warren, S. J. 2009, MNRAS, 394, 675
Irwin, M. J., Lewis, J., Hodgkin, S., et al. 2004, in Optimizing Scientific Return for Astronomy through Information Technologies. eds. P. J. Quinn, & A. Bridger, 5493, 411
Lauger, S., Burgarella, D., & Buat, V. 2005, A&A, 434, 77
Lintott, C. J., Schawinski, K., Slosar, A., et al. 2008, MNRAS, 389, 1179
Lintott, C., Schawinski, K., Bamford, S., et al. 2011, MNRAS, 410, 166
Lotz, J. M., Primack, J., & Madau, P. 2004, AJ, 128, 163
Merluzzi, P., Mercurio, A., Haines, C. P., et al. 2010, MNRAS, 402, 753
Molinaro, M., Knapic, C., & Smareglia, R. 2012, in Software and Cyberinfrastructure for Astronomy II, Proc. SPIE, 8451, 12
Nair, P. B., & Abraham, R. G. 2010, ApJS, 186, 427
Omizzolo, A., Fasano, G., Reverte Paya, D., et al. 2014, A&A, 561
Pahre, M. A. 1999, ApJS, 124, 127
Pignatelli, E., Fasano, G., & Cassata, P. 2006, A&A, 446, 373
Scarlata, C., Carollo, C. M., Lilly, S., et al. 2007, ApJS, 172, 406
Shamir, L. 2009, MNRAS, 399, 1367
Smith, G. P., Haines, C. P., Pereira, M. J., et al. 2010, A&A, 518, L18
Taylor, M. 2005, Astronomical Data Analysis Software and Systems XIV, ASP Conf. Ser., 347
Tody, D., Plante, R., & Harrison, P. 2011 [arXiv:1110.0499]
Valentinuzzi, T., Woods, D., Fasano, G., et al. 2009, A&A, 501, 851
van der Wel, A. 2008, ApJ, 675, L13
Varela, J., D'Onofrio, M., Marmo, C., et al. 2009, A&A, 497, 667
Vulcani, B., Poggianti, B. M., Fasano, G., et al. 2012, MNRAS, 420, 1481
Willett, K. W., Lintott, C. J., Bamford, S. P., et al. 2013, MNRAS, 435, 2835
Williams, R., Hanisch, R., Szalay, A., & Plante, R. 2011 [arXiv:1110.0498]